Kuwait J.Sci., Vol.50, No.(3B),July.2023,pp(1-9)

Investigation of V_2O_5-$ZnAl_2O_4$ composite nanoparticles for C-band microstrip patch antenna applications

Srilali Siragam[1], R.S. Dubey [2,3,*], Lakshman Pappula [4]

[1]*Dept. of ECE, Swarnandhra College of Engineering & Technology, Narsapur-534 280, West Godavari (AP), India*

[2]*University Institute of Engineering & Technology, Guru Nanak University, Ibrahimpatnam, R. R. District, Hyderabad-501 506 (T.S.), India*

[3]*Dept. of Electronics & Communication Engineering, Guru Nanak Institutions Technical Campus,Ibrahimpatnam, R. R. District, Hyderabad, (T.S.), India*

[4]*Dept. of ECE, Koneru Lakshmaiah Education Foundation, Greenfields, Vaddeswaram, Guntur, Andhra Pradesh, India*

**Corresponding author: rag_pcw@yahoo.co.in*

Abstract

This paper reports the prototype fabrication and characterization of microstrip patch antenna using the sol-gel derived composite nanoparticles of vanadium pentoxide oxide (V_2O_5) and zinc aluminate ($ZnAl_2O_4$). The prepared composite nanoparticles were characterized using X-ray diffraction (XRD), which exhibited the dominant peaks of $ZnAl_2O_4$ and V_2O_5. The crystallite size of the nanoparticles was estimated to be 16 nm. The sample was also studied using the Fourier transform infrared spectroscopy (FTIR), field-emission scanning electron microscopy (FESEM), and energy dispersive spectroscopy (EDS) to examine the functional groups morphology and elemental composition present in the composite nanoparticles. Further, these nanoparticles were employed in fabricating the prototype microstrip patch antenna to evaluate its characteristics. The fabricated antenna showed its return loss of -17.13 dB at a resonant frequency of 4.64 GHz.

Keywords: Bandwidth ; return loss; sol-gel synthesis; vanadium oxide, zinc aluminate.

1. Introduction

Dielectric microstrip antennas have received much interest in recent microwave communications because of their small size, better radiation efficiency, and ease of excitation. A microstrip antenna material should have the following properties: i) a high Q-factor to achieve better radiation efficiency (ii) reasonably a large dielectric constant as it felicitates in a small dimension of the antenna and (iii) zero temperature coefficient of resonant frequency (Li *et al.*, 2018; Jimago *et al.*, 2020; Tachafine *et al.*, 2021). Wireless communication has become a need in occurs day to day life. This communication method is comparable to wired communication networks in terms of data rate and service quality. As technology advances, wireless communication systems must incorporate new functionalities and more components.

Zinc aluminate ($ZnAl_2O_4$) is a spinel group material that has been investigated and attracted the interest of researchers. This is due to their distinct features, which allow them to be widely used as catalyst support, ceramic material, electrical and optical materials (Kolthoum *et al.*, 2019; Khasan *et al.*, 2017; Chaudhary *et al.*, 2018; Mane *et al.*, 2020; Sommer *et al.*, 2020). Aluminum spinel has good thermal stability, a high mechanical resistance, and minimal surface acidity (Kim *et al.*, 2019). This material can be employed as a catalyst and a carrier for active metals (Younis *et al.*, 2021). The cubic cell of $ZnAl_2O_4$ comprises 32 tightly packed oxygen atoms with cations in tetrahedral and octahedral interstices. Divalent cations occupy tetrahedral positions in typical spinel structures (Santos *et al.*, 2017; Wu *et al.*, 2011). $ZnAl_2O_4$ material is commonly utilized as microwave dielectric ceramics, where it has the potential for the future study focused on microwave applications (Akkika *et al.*, 2020). Further, the properties of $ZnAl_2O_4$ can be manipulated by doping or adding desired elements for specific applications. The combination of $ZnAl_2O_4$ and V_2O_5 can facilitate the alteration of various properties. The combination of Vanadium oxide is a phase transition material with many valences. Its oxide has valence states of 2+, 3+, 4+, 5+, etc., as well as various intermediate oxide states. The phase transition temperature of each variation differs. Despite various synthesis methods such as solid-state and co-precipitate, the sol-gel method is well established to synthesize doped or composite nanoparticles (Mishra *et al.*, 2018; Dwiwedi *et al.*, 2017; Priya *et al.*, 2020; Tangchareon *et al.*, 2019). At a low-temperature process, one can produce fine, and impurity-free particles (Rahman *et al.*, 2015). Wang *et al.* (2009) employed the $(1-x)(0.79ZnAl_2O_4\text{-}0.21Mg_2TiO_4)\text{-}xSrTiO_3$ composite material in fabricating the microstrip patch antenna. The fabricated patch antenna showed its resonant frequency of 1.575 GHz with VSWR less than 2. Naidu *et al.* (2012) used the magnesium ferrite doped with double Samarium (Sm) and Dysprosium (Dy) for fabricating the microstrip patch antenna. The efficiency of the patch antenna was noticed to be 69.82 at frequency 14.9 GHz, which its gain of about 5.73 dB. Rahman *et al.* (2015) studied the patch antenna prepared using the $ZnAl_2O_4$ nanoparticles prepared by the sol-gel technique. They studied the antenna's performance and claimed its return loss of -25.4 dB at the resonant frequency of 12.78 GHz, having a bandwidth of 760 MHz. Further, they explored the application of the prepared antenna in X-band communication. Wu *et al.* (2011) prepared the dielectric ceramics of $ZnAl_2O_4$, TiO_2, and $MgTiO_3$ using gel casting. They prepared nanoparticles that exhibited their dielectric permittivity in the range from 11.75-12.25 and employed them to fabricate the GPS patch antenna, demonstrating its resonant frequency at 1.75 GHz. Wee *et al.* (2012) reported the fabrication of 2, 4, 6-element arrays of the barium strontium titanate (BST) based microstrip patch antennas. They reported the 6-element BST array antenna's enhanced gain compared to the 4-element BST antenna and suggested their applications in Wi-MAX and WLAN communications.

This work reports the synthesis of composite nanoparticles of $0.1V_2O_5\text{-}0.9ZnAl_2O_4$ using the sol-gel process. The prepared nanoparticles were employed to fabricate the microstrip patch antenna, and performance was evaluated. Section 2 presents the materials and methods of the synthesis process, and the characterized results are discussed in Section 3. At last, Section 4 concludes the work.

2. Materials and Methods

Vanadium pentoxide (V_2O_5) (LR grade), Zinc acetate $(CH_3COO)_2Zn_2H_2O$ (AR) (Lobychem), aluminum nitrate nonahydrate $(Al_2(NO_3)_3.9H_2O$, (Sigma Aldrich), ethanol (C_2H_5OH, Sigma Aldrich), ethylene glycol (EG, AR grade) and nitric acid (HNO_3) (AR) were used with any further purification.

For preparing the composite nanoparticles of $xV_2O_5(1\text{-}x)ZnAl_2O_4$, the molar concentration x=0.1 was chosen. Initially, 37.5 gm $Al_2(NO3)_3.9H_2O$ was dissolved in 100 ml ethanol under constant stirring. After this, 1 ml of ethanediol was added to the above solution and stirred for 5 minutes. Subsequently, 1 gm and 16.53 gm of V_2O_5 powder and $(CH_3COO)_2Zn2H_2O$ were added to the above solution. The stirring was maintained at a temperature of 75 ^{O}C for 60 min. Later, 0.6 ml HNO_3 was added to get the homogeneous solution. After obtaining the transparent solution of $0.1V_2O_5\text{-}0.9ZnAl_2O_4$, it was kept for drying to get powder. Finally, the prepared powder was calcined at a temperature of 800 ^{O}C for 1 hr and ground to obtain a fine powder.

3. Results and Discussion

Figure 1 depicts the XRD pattern of prepared $0.1V_2O_5\text{-}0.9ZnAl_2O_4$ composite nanoparticles calcinated at 800 °C for 1 hr, showing the polycrystalline phase. The peaks regarded the $ZnAl_2O_4$ crystal structure, which indicated the typical face-centered cubic shape and was found inconsistent with the reported work (Ding *et al.*, 2017; Dubey *et al.*, 2020; Siragam *et al.*, 2020). The XRD pattern shows the dominant peaks of $ZnAl_2O_4$ at 2Θ= 31.26°, 35.02, 37.09°, 44.98°, 49.29°, 55.93°, 59.57°, 65.38°, 74.30° and 77.57° corresponding to the planes (220), (101), (311), (400), (311), (422), (511), (440), (620) and (533) which shows matching with the JCPDS card No. 00-005-0669.

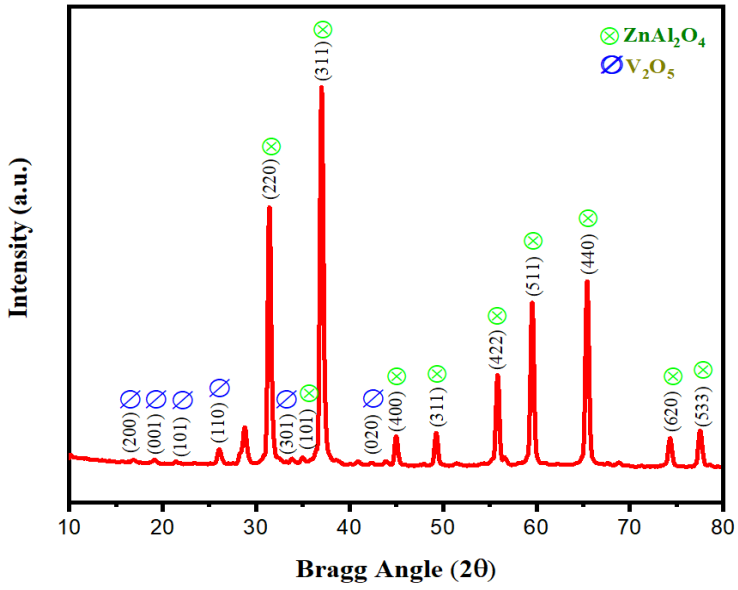

Fig. 1. XRD pattern of $0.1V_2O_5\text{-}0.9ZnAl_2O_4$ composite nanoparticles.

Furthermore, V_2O_5 peaks were noticed at 2θ=16.86°, 19.06°, 21.55°, 26.11°, and 33.78° corresponding to the planes (200), (001), (101), (110) and (301), respectively. These diffraction peaks were found in good matching with the ICPDS file 98-000-6037 and well-matched with the previous works (Chan *et al.*, 2014)[23]. The crystallite size of the $0.1V_2O_5$-$0.9ZnAl_2O_4$ sample was estimated to be 16 nm as calculated by using Scherrer's equation.

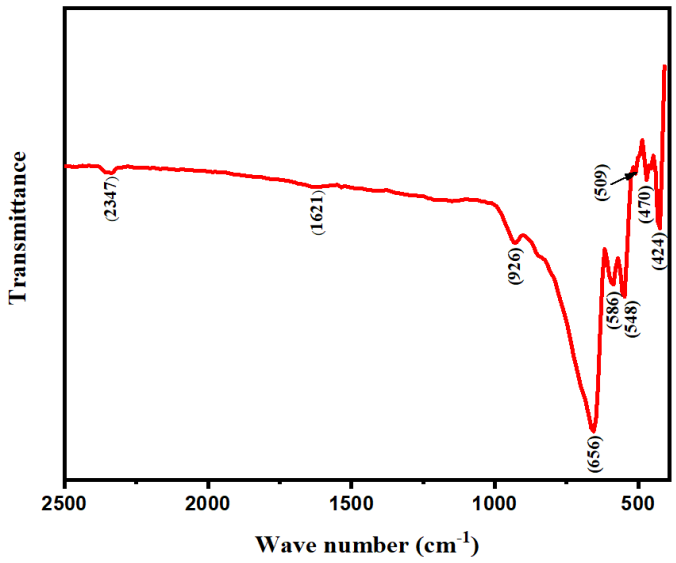

Fig. 2. FTIR spectra of $0.9ZnAl_2O_40.1V_2O_5$ composite nanoparticles.

FTIR investigation was done to know the functional groups in the prepared nanoparticles. Figure 2 depicts the FTIR spectrum of the composite nanoparticles plotted in the range 2500-400 cm^{-1}. The FTIR transmittance peak associated at wavenumbers 470, 586 cm^{-1} are ascribed to the V_2O_5, V_2O_3 bands (Fatmeh *et al.*, 2011;). A peak observed at 509 cm^{-1} corresponds to the stretching vibration of $ZnAl_2O_4$. Further, the peaks aligned at 548 and 656 cm^{-1} are regarded as ZnO's stretching vibrations and AlO (Muhmmad *et al.*, 2011). Another peak originated at 1621 cm^{-1} is associated with the stretching vibrations of O-H, i.e., related to H_2O molecules. We can also notice the O-O band vibration peak at 2348 cm^{-1} related to the FCC crystal lattice of O_2 atoms (Henam *et al.*, 2021).

Figure 3 (a) depicts the SEM morphology of the $0.1V_2O_5$-$0.9ZnAl_2O_4$ particles, which shows the formation of agglomerated spherical composite nanoparticles. The mean diameter of nanoparticles was observed to be 21 nm. EDS spectroscopy was carried out to know the presence of constituting elements present in the prepared sample. Figure 3(b) chooses the spectrum, which reveals the elemental compositions of Zn, Al, O, and V at 1.5, 1, 0.5, and 5 KeV, respectively.

We have fabricated the prototype of a microstrip patch antenna using the prepared composite nanoparticles, which were cast on the FTO substrate. Later, the silver coating was done on both sides of the FTO for the contacts. The co-axial SMA connector was connected to complete the fabrication of the microstrip patch antenna.

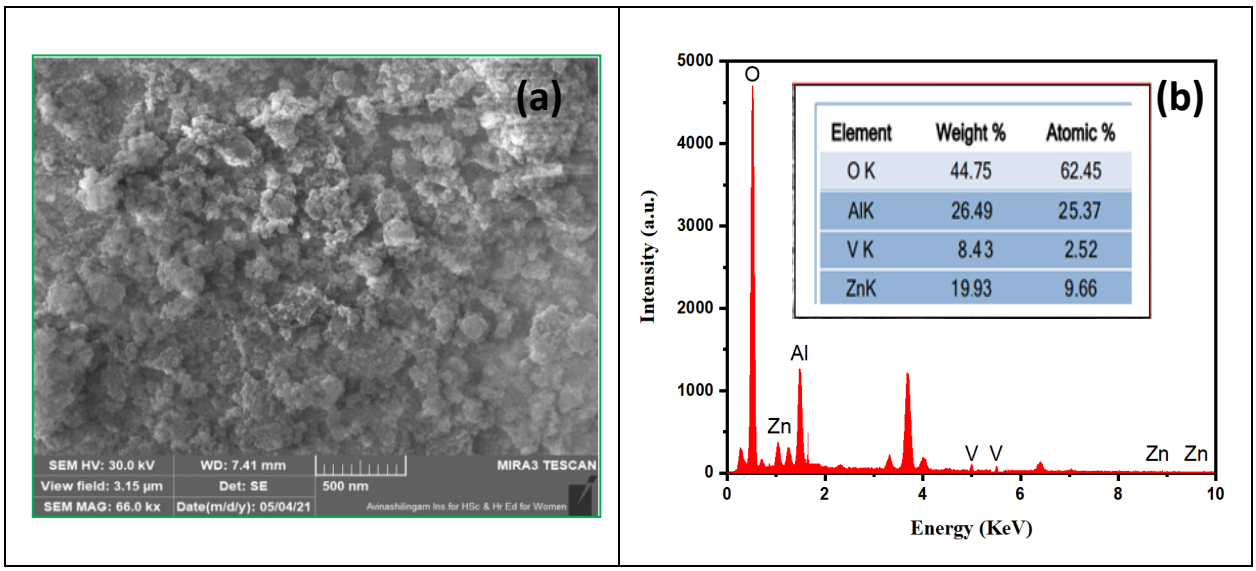

Fig. 3. (a) SEM morphology of $0.1V_2O_5$-$0.9ZnAl_2O_4$ (b) EDS spectrum.

Figure 4 depicts the return loss (RL) from 3-6 GHz of the fabricated antennas with respect to the operating frequency. We can notice the return loss of -17.13 dB at the resonant frequency of 4.64 GHz. In a similar work, Thirumanathan *et al.* (2016) reported the performance of a patch antenna made up of $Bi_4Ti_3O_{12}$ composite metal and claimed its return loss of -4.95 dB at resonant frequency 2.45 GHz for wireless communication applications. Our microstrip patch antenna based on $0.1V_2O_5$-$0.9ZnAl_2O_4$ composite nanoparticles evidenced the better return loss. Therefore, it was found suitable in C-band communication. To the best of our knowledge, no such work of microstrip patch antenna based on V_2O_5-$ZnAl_2O_4$ has been reported. The inset of figure 4 shows the digital picture of the microstrip patch antenna with its dimension 2.5×1.5 cm^2.

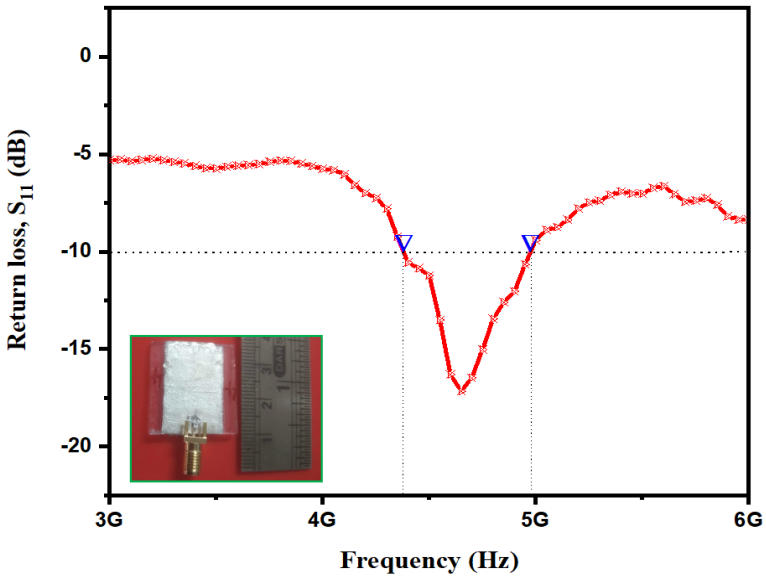

Fig. 4. Return loss of $0.1V_2O_5$-$0.9ZnAl_2O_4$ microstrip patch antenna.

The voltage standing wave ratio (VSWR) value is directly connected to the maximum power transmitted from the transmitter to receiving antenna in an ideal condition. This occurs only when the input impedance is matched to the transmitting antenna impedance. We can calculate the VSWR value using the expression $VSWR = V_{max}/V_{min} = (1 + |\rho|)/(1 - |\rho|) = (1 + S_{11})/(1 - S_{11})$. Accordingly, we have plotted the obtained VSWR values and reflection coefficient as shown in figure 5 as the reflected and forwarded powers of microstrip patch antenna were 1.92% and 98.07%, respectively.

At the resonant frequency of 4.64 GHz, the VSWR value of the microstrip patch antenna was found to be 1.32. In general, VSWR affects the reflection coefficient of the antenna under the test, and a larger ratio (V_{max}/V_{min}) implies a severe mismatch rather than a perfect matching (i.e., 1:1 ratio). The maximum and minimum amplitudes of the standing wave cause this match/mismatch. The obtained VSWR value is less than 2, favorable to a better return loss, as depicted in figure 5 (left axis). The microstrip patch antenna's reflection coefficient was 0.13, as shown in figure 5 (right axis). Finally, the estimated antenna's mismatch loss was 0.083 dB, whereas the reflected and forwarded powers of the microstrip patch antenna were 1.92% and 98.07%, respectively.

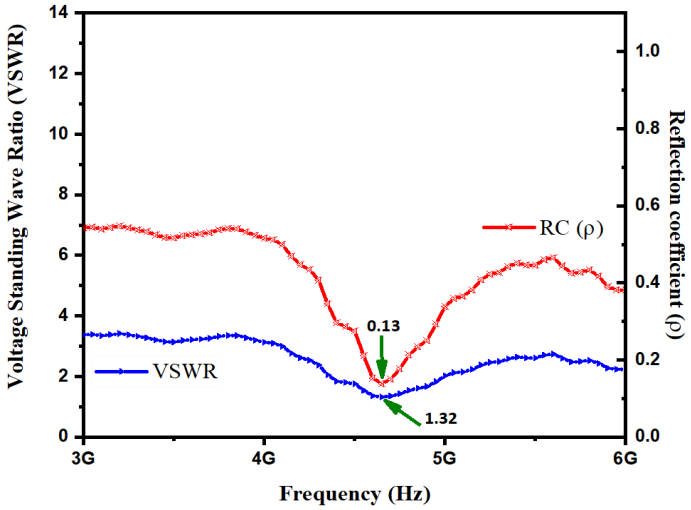

Fig. 5. VSWR & Reflection coefficient of $0.1V_2O_5$-$0.9ZnAl_2O_4$ microstrip patch antenna.

4. Conclusions

Synthesis of $0.1V_2O_5$-$0.9ZnAl_2O_4$ composite nanoparticles prepared by the sol-gel method is presented and analyzed. XRD pattern revealed the preparation of crystalline nanoparticles with their crystallite size of 16 nm. The presence of diffraction peaks of V_2O_5 and the dominant peak of $ZnAl_2O_4$ confirmed the synthesis of composite nanoparticles. The FTIR investigation evidenced various vibration peaks related to the functional groups. The FESEM micrograph confirmed the growth of the agglomerated spherical nanoparticles having theirs mean diameter of 21 nm. The EDX spectroscopy also affirmed the presence of Al, Zn, O, and V at 1.5, 1, 0.5, and 5 KeV, respectively. Further, we have fabricated the microstrip patch antenna, which demonstrated the

return loss of -17.13 dB at the resonant frequency 4.64 GHz, while the VSWR value was observed to be less than 2. The performance of the microstrip patch antenna based on $0.1V_2O_5$-$0.9ZnAl_2O_4$ composite nanoparticles signify the applications in C-band communication.

References

A, Tachafine., D, Fasquelle., R, Desfeux., A, Ferri., A, Da Costa., J,-C, Carru., & A, Outzourhit. (2021) Doping effect on nanoscopic and macroscopic electrical properties of Barium Zirconate Titanate thin films. Spectroscopy Letters, 54(7): 507–519.

Akika, F.Z., Benamira, M, Lahmar H., Trari, M., Avramova, I., Suzer, Ş. (2020) Structural and optical properties of Cu-doped $ZnAl_2O_4$ and its application as photocatalyst for Cr (VI) reduction under sunlight. Surfaces and Interfaces, 18, 100406–100440.

Chan, Yim-Leng., Pung, Swee-Yong., Sreekantan, Srimala. (2014). Synthesis of V_2O5 Nanoflakes on PET Fiber as Visible-Light-Driven Photocatalysts for Degradation of RhB Dye. Journal of Catalysts, 1–7.

Chaudhary, Archana., Mohammad, Akbar., Mobin, Shaikh, M. (2018) Facile synthesis of phase pure $ZnAl_2O_4$ nanoparticles for effective photocatalytic degradation of organic dyes. Materials Science and Engineering: B, 227: 136–144.

Ding, Jijun., Chen, Haixia., Fu, Haiwei. (2017) Enhanced blue emission of ZnO films deposited on AlN substrates. Physica E: Low-dimensional Systems and Nanostructures, 90: 61–66.
Dubey, R.S. (2018) Temperature-dependent phase transformation of TiO_2 nanoparticles synthesized by sol-gel method. Materials Letters, 215: 312–317.

Dwibedi, Debasmita., Murugesan, Chinnasamy., Leskes, Michal., Barpanda, Prabeer. (2017) Role of Annealing Temperature on Cation Ordering in Hydrothermally Prepared Zinc Aluminate ($ZnAl_2O_4$) Spinel. Materials Research Bulletin, 98: 219-224.

E, Muhammad Abdul Jamal., D, Sakthi kumar., and M, R, Anantharaman. (2011) On structural, optical and dielectric properties of zinc aluminate nanoparticles. Bull. Mater. Sci., 34 (2): 251–259.

Fatemeh, Davar., Masoud, Salavati-Niasari. (2011) Synthesis and characterization of spinel-type zinc aluminate nanoparticles by a modified sol–gel method using new precursor. Journal of Alloys and Compounds, 509: 2487–2492.

Henam, Sylvia Devi., Akshita, Mishra., Md, Samim Reza., Parvez, Akhtar., Henam, Premananda Singh., Thiyam, David Singh., Madhusudan, Singh. (2021) Controlled phase synthesis of V_mO_n in differing oxidation states using a simplified formic acid process, quantified with a new generalized index designed for use with public domain material process information. Green Chem., 23: 8200-8211.

Jiamao, Li., Zhang, Chuimin., Li, Lin., Fan Chuangang. (2020) Synthesis of $NdAlO_3$ with good microwave dielectric properties by stearic acid method. Ceramics International, 46 (11): 18940–18947.

Khasan, S. Karimov., Muhammad, Saleem, Khakim., M. Akhmedov., Taimoor, Ali. Muhammad M. (2017) BashirPhoto-thermo electric effect in Zn/orange dye aqueous solution/carbon cell. Kuwait J. Sci., 44 (1): 86-90.

Kim, Hyo-Young., Shin, Jeeyoung., Jang, Il-Chan., Ju, Young-Wan. (2019) Hydrothermal Synthesis of Three-Dimensional Perovskite $NiMnO_3$ Oxide and Application in Supercapacitor Electrode. Energies, 13(1): 36–47.

Kolthoum, I Othman., M, EI Sayed Ali., and S.EI Hout. (2019) Dielectric properties of sintered $BaTiO_3$ prepared from barium acetate and titanium dioxide. Kuwait J. Sci., 46(3): 53-59.

Li, Wei., Qu, Jing-Jing.,Wei, Xing., Liu, Fei., Yuan, Chang-Lai., Chen, Guo-Hua. (2018) Structural characteristics and microwave dielectric properties of a new Sm_2O_3- Nd_2O_3-MgO-CeO_2 ceramic system. Materials Chemistry and Physics, 207: 44–49.

Mane, Chandrakant B., Pawar, Ramkrushna P., Patil, Rajendra P., Patil, Sarjerao B. (2020) Photocatalytic Environmental Remediation of Cassiteriteâ□Titania Nanocomposite. Macromolecular Symposia, 393(1): 2000176.

Mishra, Geetanjali., Dash, Barsha., Pandey, Sony. (2018) Layered double hydroxides: A brief review from fundamentals to application as evolving biomaterials. Applied Clay Science, 153: 172–186.

Naidu, V., Ahamed, Kandu Sahib S. K. A., Sivabharathy, M., Legadevi R, Senthil Kumar A., Prakash C., & Pandian, S. (2012) Synthesis and Characterization of Novel Nanoceramic Magnesium Ferrite Material Doped with Samarium and Dysprosium for Designing – Microstrip Patch Antenna. Defect and Diffusion Forum, 332: 35–50.

Priya, Ruby., Negi, Astha., Singla, Shivani., Pandey, O.P. (2020) Luminescent studies of Eu doped $ZnAl_2O_4$ spinels synthesized by low-temperature combustion route. Optik, 204:164173–164184.

Rahman, A., Islam, M. T., Zulfakar, M. S., & Abdullah, H. (2015) Synthesis and characterization of gahnite-based microwave dielectric ceramics (MDC) for microstrip antennas prepared by a sol–gel method. Journal of Sol-Gel Science and Technology, 74(2): 557–565.

Santos, J.L., Reina, T.R., Ivanova, S., Centeno, M.A., Odriozola, J.A. (2017) Gold promoted $Cu/ZnO/Al_2O_3$ catalysts prepared from hydrotalcite precursors: Advanced materials for the WGS reaction. Applied Catalysis B: Environmental, 201: 310–317.

Siragam, S., Dubey, R. S., & Pappula, L. (2020) Synthesis and investigation of dielectric properties of nanoceramic composite material for microwave applications. Micro & Nanoletters, 15 (15): 1156 –1161.

Sommer, S., Bøjesen, E. D., Reardon, H., & Iversen, B. B. (2020) Atomic scale design of spinel $ZnAl_2O_4$ nanocrystal synthesis. Crystal Growth & Design, 1789-1799.

Tangcharoen, T., T-Thienprasert., J & Kongmark, C. (2019) Effect of calcination temperature on structural and optical properties of MAl_2O_4 (M = Ni, Cu, Zn) aluminate spinel nanoparticles. J Adv Ceram, 8: 352–366.

Thiruramanathan., Sanjeev, K. Sharma., S, Sankar., R. Sankar. Ganesh., A. Marikani., Deuk, Young, Kim. (2016) Synthesis of bismuth titanate (BTO) nanopowder and fabrication of microstrip rectangular patch antenna. Appl. Phys. A, 122:1006.

Wang, X., Lei, W., & Lu, W. (2009) Novel $ZnAl_2O_4$-Based Microwave Dielectric Ceramics with Machinable Property and its Application for GPS Antenna. Ferroelectrics, 388(1): 80–87.

Wee, F.H., Malek F., Ghani, F., Sreekantan, S., Al-Amani, A.U. (2012) High gain and high directive of antenna arrays utilizing dielectric layer on bismuth titanate ceramics. Int. J. Antennas Propag, 1–8.

Wu, J-M., Lu, W-Z., Lei, W., Wang, X-C. (2011) Preparation of $ZnAl_2O_4$-based microwave dielectric ceramics and GPS antenna by aqueous gelcasting. Mater Res Bull, 46(9):1485–1489.

Younis, N., Abd-Elrahman, M. I., Afify, N., Abu El-Fadl, A., & Abu-Sehly, A. A. **(2021)** Structural, optical and magnetic characterizations of nanoparticles spinel $Zn_{(1-x)}M_xAl_2O_4$(M=Co and Ni) synthesized by microwave combustion method. Materials Science and Engineering: B, 271: 115316.

Submitted: 18/12/2021
Revised: 26/02/2022
Accepted: 26/02/2022
DOI : 10.48129/kjs.17783